Stacked Structure of the Glycine Dimer Is More Stable than the Cyclic Planar Geometry with Two O−H···O Hydrogen Bonds: Concerted Action of Empirical, High-Level Nonempirical ab Initio, and Experimental Studies

Jana Chocholoušová, Jaroslav Vacek, Friedrich Huisken,† Olav Werhahn,† and Pavel Hobza*

J. Heyrovský Institute of Physical Chemistry, Academy of Sciences of the Czech Republic and Center for Complex Molecular Systems and Biomolecules, Dolejškova 3, 182 23 Prague, Czech Republic, and Max-Planck-Institut für Strömungsforschung, Bunsenstrasse 10, D-37073 Göttingen, Germany

Received: April 10, 2002; In Final Form: September 4, 2002

The potential energy surface of the glycine dimer was investigated by the molecular dynamics/quenching method. A new empirical potential (EP1), largely based on the standard AMBER force field of Cornell et al. (Cornell, W. D.; Cieplak, P.; Bayly, C. I.; Gould, I. R.; Merz, K. M.; Ferguson, D. M.; Spellmeyer, D. C.; Fox, T.; Caldwell, J. E.; Kollman, P. *J. Am. Chem. Soc.* **1995**, *117*, 5179), was introduced. It employs atomic polarizabilities and RESP/B3LYP/aug-cc-pVTZ atomic charges and well mimics the high-level ab initio PES of the glycine dimer. Surprisingly, the most stable structure of the glycine dimer determined with the EP1 potential does not correspond to the planar cyclic structure with two O−H···O hydrogen bonds (C1) but to a stacked arrangement (S1). The stabilization energies of the 22 lowest-energy isomers of the glycine dimer were recalculated at the MP2/6-31G** level of theory, and the largest difference was found for the C1 and S1 structures. While the empirical potential favored the S1 structure by 3 kcal/mol, the correlated ab initio MP2/6-31G** calculations preferred the C1 structure by 2 kcal/mol. Applying higher levels of ab initio calculations (countrepoise corrected gradient optimization, larger basis sets, CCSD, CCSD(T), and QCISD(T) methods), we found that both structures are comparable in energy or that the stacked structure is even slightly more stable. The finding that the cyclic C1 structure is not the lowest energy configuration is in good agreement with IR spectroscopic studies on glycine dimers trapped in liquid helium droplets. All experimental spectra feature a strong absorption band in the region of the free O−H stretch, indicating that both hydroxyl groups cannot be hydrogen-bonded in the glycine dimer at the same time. Due to fast (subnanosecond) cooling of the glycin dimer in the helium droplets, it is also suggested that a T-shaped local minimum can be preserved in the cluster.

I. Introduction

Amino acids and proteins are among the most important biological systems. The simplest amino acid, glycine, is known to exist in solution and in the crystalline phase as zwitterion $NH_3-CH_2^+-COO^-$ while, in the gas phase, it appears in the nonionized form NH_2-CH_2-COOH. The specific behavior of glycine (as well as of any other amino acid) is determined by its great flexibility, which is due to the rotation around the three axes going through the N−C, C−C, and C−O bonds. For this reason, its potential energy surface (PES) looks like a landscape with many hills and valleys of different heights and depths, and the determination of the global minimum represents a rather difficult task. The situation is even more complicated in the case of the glycine dimer because the global minimum can be realized not only through the interaction of monomers in their lowest energy structure but also through interaction of monomers in any other conformeric structure with higher energy. The energy increase (due to passage from the global minimum to a local minimum) can be compensated by the gain in a more favorable interaction energy. Evidently, very efficient searching procedures should be adopted to scan the whole PES, and it is impossible to rely on chemical experience or chemical intuition alone. These methods are usually based on computer simulations, and it is mainly the molecular dynamics (MD) which is used. Localization of all stationary points of the PES is beyond the capability of ab initio techniques and must be done using an empirical potential. Ab initio calculations are then used to verify the quality of the empirical force field. It is clear that the combination of an inaccurate empirical force field and high-level computer simulations will lead to inaccurate results as well.

The glycine monomer was intensively studied theoretically[1−3] at various levels of ab initio theory and also experimentally.[4,5] Ab initio methods describe the PES at 0 K, but experiments are performed at finite temperature. Therefore, in some cases, the entropy needs to be considered. This means that it is necessary to pass from the energy description to the free energy description. Only if the experiments are performed at very low temperatures which are close to 0 K then it is sufficient to work on the PES. The temperature in rare gas matrixes is rather low, between 5 and 20 K. A considerably lower temperature, however, is reached in helium droplets. This rather new technique, which is applied in the present experimental study, yields a temperature as low as 0.4 K. Thus, the experimental results can be directly compared with the theoretical PES data. To the best of our knowledge neither nonempirical ab initio studies nor experimental gas-phase, helium droplet, or rare gas matrix studies on the glycine dimer have been reported up to

* To whom correspondence should be addressed. E-mail: hobza@indy.jh-inst.cas.cz. Fax: +420-2-8658-2307.
† Max-Planck-Institut für Strömungsforschung.

10.1021/jp025925a CCC: $22.00
Published on Web 11/05/2002

now. However, experiments in a solvent of week polarity have been performed for N−t-BOC glycine and formation of homodimers and heterodimers has been demonstrated.[6] Besides determining the PES of the dimer and comparing the PES results with the experimental data obtained in helium droplets, we will also evaluate the free energy surface of the dimer with the aim to study the role of entropy on the structure of the dimer.

The easiest way to determine the entropy and free energy is to use the rigid rotor-harmonic oscillator-ideal gas approximation (RR−HO−IG). However, for floppy systems, this approximation is of limited use and statistical methods and computer experiments will play a key role here. The RR−HO−IG calculations require the knowledge of the total partition function and the value of the standard entalpy at 0 K (H_0^0). The values are determined by means of quantum chemistry.

The purpose of the present theoretical study is 3-fold: first, to develop an empirical potential function which describes correctly the relative energies of the stationary points on the PES of glycine; second, to investigate the PES and FES of glycine; third, to apply the empirical potential function to the glycine dimer, to study which regions of the PES and FES are explored, and to establish whether present-day ab initio methods are able to reproduce experimental results on the glycine dimer trapped in helium droplets.

II. Strategy of Calculation

The potential energy surface of the glycine monomer was searched employing the molecular dynamics/quenching technique[7] using a newly developed empirical force field (EP1) based on the standard potential of Cornell et al.[8] To describe the relative energies of various newly introduced energy minima correctly, it was necessary to use high-level atomic charges as well as to introduce the polarization term. Despite the use of these charges and the inclusion of the polarization term, the agreement between the relative energies of the ab initio second-order Møller−Plesset method (MP2) and those obtained with the empirical potential was still not satisfactory. The final tuning was reached by fitting the torsional barriers belonging to the angles H−N−C−C, N−C−C−O, and O−C−C−OH.

The PES of the glycine dimer was investigated by the MD/quenching method[7−9] utilizing the empirical force field mentioned above. The relative dimer energies obtained with the empirical potential were then compared with the correlated ab initio energies.

III. Methods

A. Ab Initio Quantum Chemical Calculations. The geometries of different glycine stationary points were optimized at the correlated ab initio MP2/6-31G** and MP2/aug-cc-pVDZ levels. All structures of the glycine dimer were optimized at the MP2/6-31G** level and selected structures also at the MP2/aug-cc-pVDZ and the RI-MP2/TZVPP[10−12] (resolution of the identity MP2) levels. Because the 6-31G** basis set underestimates the dispersion attraction essential for the description of stacked structures, the stabilization energies for the optimized dimer structures were also calculated at MP2/6-31G*(0.25) level, i.e., using a basis set with more diffuse polarization functions. This means that the standard exponent of the polarization d-functions (0.8) is replaced by the more diffuse value of 0.25. Final stabilization energies were corrected for the basis set superposition error (BSSE)[13] and the deformation energies of the monomers (see ref 9 for details).

Usually, the BSSE correction is added a posteriori at the end of the optimization of the complex. This means that the structure is optimized on the standard PES and not on a theoretically more justified counterpoise (CP)−corrected PES. The CP-corrected optimization[14,15] includes the BSSE correction in each optimization step and is therefore more reliable. Unfortunately, due to the very slow convergence, the CP-corrected optimization is significantly more time-demanding. Therefore, the CP-corrected optimization was only employed for the two lowest glycine dimer structures.

Harmonic vibrational frequencies were determined at the MP2/6-31G** level. The ab initio thermodynamic characteristics were evaluated within the rigid rotor−harmonic oscillator−ideal gas approximation.

All calculations were performed using the GAUSSIAN 98 [16] and Turbomol[17] codes except for the CP-corrected optimizations that were done with our own program.[15]

B. Empirical Potential EP1. A new force field (denoted EP1) was constructed by modifying the standard force field of Cornell et al.[8] to mimic the relative energies of the five lowest energy minima of the glycine monomer determined at the MP2/aug-cc-pVDZ level. The polarization term was included to improve the empirical potential function and to consider the dynamical behavior of conformational changes. The atomic charges on the glycine molecule are strongly conformation-dependent and thus force fields with constant atomic charges and without polarization term do not provide a correct description of the PES. Atomic polarizabilities of Applequist were used. [18]

Partial atomic charges were determined using the two-stage multiple conformation restrained electrostatic potential (RESP)[19] fitting procedure. Atomic charges used in the potential of Cornell et al.[8] are standardly calculated at the RESP/HF/6-31G* level. The resulting molecular dipole moments are overestimated by about 12% compared to gas phase experimental dipole moments. The HF/6-31G* charges are successfully used for calculations in a water environment, where the overestimated electrostatic energy compensates the missing polarization term.[20,21] Because the polarization term is explicitly taken into account, it is advisable to use charges that are in vacuo as accurate as possible.[20] The present atomic charges (potential EP1) were therefore determined using the RESP/DFT/B3LYP/aug-cc-pVTZ method.

The use of original van der Waals parameters for HO type hydrogen ($R^* = 0.0000$ Å; $\epsilon = 0.0000$ kcal/mol) led to numerically unstable MD simulations sometimes referred to as "polarization catastrophe" for the glycine dimer. Therefore, HO radius (R*) and its potential well depth (ϵ) were set to 0.3000 Å and 0.0057 kcal/mol, respectively. Finally, the values of the torsional barriers for the CT-C−OH−HO, O−C−CT−N3, and C−CT-N3−H angles were adjusted to achieve reasonable correspondence between the MP2/aug-cc-pVDZ and the empirical EP1 potential.

C. Molecular Dynamics/Quenching/EP1 Calculations. Constant-energy MD/QUENCHING (MD/Q) simulations (NVE ensemble) and empirical potential EP1 were used to study nonrigid dynamics of glycine monomers. The respective procedure is described in detail elsewhere.[7,9] To estimate the PES of glycine, i.e., to localize all relevant energy minima, relatively short MD simulations suffice while rather long simulations ($\sim\mu$s) are required to accurately calculate the relative populations from quenching. The convergence of the MD/Q algorithm was checked by splitting the MD simulation into three parts and evaluating the populations separately in these intervals. The simulation is considered converged when the populations do not change significantly with increasing simulation time. MD simulations for the glycine monomer and dimer were performed

at constant total energies of 36.0, 39.5, 42.8, 44.8, and 47.3 kcal/mol (corresponding to average temperatures of 200, 250, 300, 350, and 400 K) and of 71.3, 77.1, 82.9, 88.5, and 93.8 kcal/mol (corresponding to the same set of average temperatures), respectively.

In the present study, the MD simulations were run with 1.0 fs time step for the glycine monomer and 0.1 fs time step for the glycine dimer. A quench (gradient geometry optimization) was performed every 20 ps for the monomer and every 10 ps for the dimer. The total MD simulation time was 1.2 μs for the glycine monomer and 0.6 μs for the dimer. The system is described by relative population numbers, indicating the relative abundance of one conformation with respect to the others, and by the number of interconversions, i.e., transitions between different structures. The error in determining the populations decreases with increasing number of interconversions.

Modified AMBER[21] package of programs was used for all MD/Q simulations.

D. Experimental Results. The experiments have been carried out at the Max-Planck-Institut für Strömungsforschung in Göttingen in a molecular beam machine that has been described in detail earlier.[22] Briefly, large helium clusters (or small helium droplets) He_N were produced by expanding helium gas at high pressure ($p_0 = 40$ bar) through a 5-μm-diam pinhole nozzle kept at low temperature ($T_0 = 12$ or 14 K). The average helium cluster size produced under these conditions was $\langle N \rangle = 15\,000$ or 11 000, respectively. After skimming, the cluster beam was directed through a heated cell in which commercial glycine (Gly) powder was evaporated at a temperature of $T_{Gly} = 120$ °C. Upon collisions, glycine molecules were picked up by the helium clusters and incorporated into their interior. The complexes formed in this way are denoted by Gly@He_N (the @ indicates that the Gly molecule is located inside the liquid helium droplet). As the mass spectrometric analysis has shown, the glycine vapor pressure is sufficiently high that multiple collisions may occur leading to the incorporation of two glycine molecules and to the formation of glycine dimers within the helium clusters (Gly_2@He_N). The kinetic and internal energy of the incorporated molecules as well as the dimer formation energy are released on a short time scale (<1 ns) by evaporating a few hundred helium atoms. This fast evaporative cooling leads to a well-defined temperature of 0.4 K within the chromophore-containing helium clusters.[23]

To study the spectroscopy of the glycine dimer in the range between 3000 and 3800 cm^{-1}, the cluster beam was subjected to the pulsed infrared (IR) radiation originating from a Nd:YAG-laser-pumped optical parametric oscillator (OPO).[24] The absorption of IR photons by the Gly_2@He_N complex results in the evaporation of another few hundred helium atoms. This process is monitored as a depletion signal with the quadrupole mass spectrometer detector into which the cluster beam is directed. Measuring the depletion on a specific mass as a function of laser frequency, an absorption spectrum of the molecule or complex responsible for the signal on this specific mass is recorded.

IV. Results and Discussion

A. Glycine Monomer. *Empirical Potential EP1.* The final monomer atomic charges were derived from electrostatic potential calculated at the DFT/B3LYP/aug-cc-pVTZ level using the multiconformation RESP fit and considering the structures Ip, IIn, and IIIn (cf. Figure 1 and Figure 2). The resulting charges together with the used AMBER atom types are reported in Figure 1. The new parameters for the dihedral angles (CT−C−OH−HO, O−C−CT−N3, and C−CT−N3−H), which are necessary to reproduce the AMBER calculations, are summarized in Table 1.

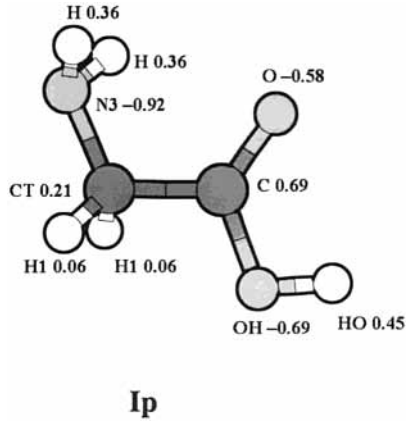

Figure 1. Global minimum of glycine Ip with EP1 atomic charges and AMBER atom types.

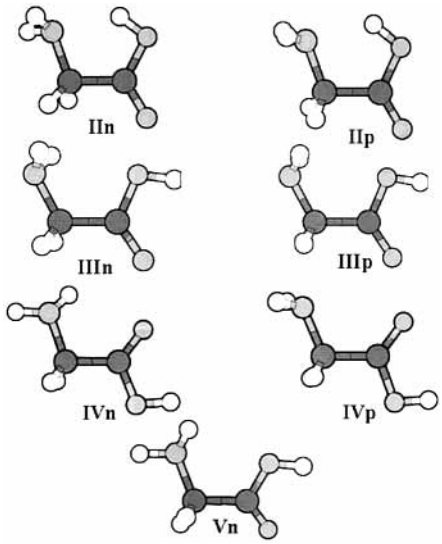

Figure 2. Structures of local minima and saddle points of glycine (p and n denote structures with planar and nonplanar heavy atom arrangement, respectively).

TABLE 1: EP1 Dihedral Parameters for Glycine

	IDIVF	PK	PHASE	PN
CT−C−OH−HO	1	1.30	180.	1.
O−C−CT−N3	1	0.77	180.	1.
C−CT−N3−H	2	0.50	0.0	1.

Potential Energy Surface. Twelve structures were localized at the PES using the MD/Q method. Only the five lowest energy minima were further considered in this study. Their structures and relative energies are reported in Figure 1, Figure 2, and Table 2, respectively. Passing from MP2/6-31G** to MP2/aug-cc-pVDZ, the relative energies are reduced and the order of isomers IIIn and IVn is also changed. This result is in accord with other published theoretical data.[1]

The EP1 and ab initio MP2/aug-cc-pVDZ data agree on structures and relative energies of the global and first local minima. For higher-energy isomers, the EP1 relative energies are lower than those from the MP2/aug-cc-pVDZ calculations. It should be stressed that the relative energies for all five lower energy isomers (Figure 1, Figure 2, and Table 2) are in good agreement with the MP2/aug-cc-pVDZ values. This finding is of key importance for subsequent empirical potential studies

TABLE 2: Relative Energies (in kcal/mol) of the Glycine Monomer Obtained by ab Initio MP2/Aug-cc-pVDZ and Empirical Potential EP1 Calculations

structure[a]	MP2/aug-cc-pVDZ ΔE	MP2/aug-cc-pVDZ ΔG	EP1 ΔE
Ip	0	0	0
IIn	0.535	1.070	0.531
IIIn	1.591	1.118	1.023
IVn	1.247	1.439	0.918
Vn	2.429	2.588	1.570

[a] cf. Figures 1 and 2, p and n denote structures with planar and nonplanar heavy atoms arrangement, respectively.

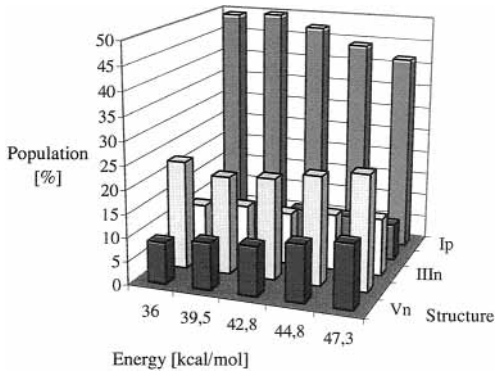

Figure 3. 3D histogram of populations of various glycine isomers (cf. Figures 1 and 2) as a function of MD total energy estimated by the MD/Q method on the EP1 PES.

of the glycine dimer. Let us mention that without introducing the polarization term we were unable to reach agreement between the emprirical potential and MP2 relative energies of the glycine monomer.

Free Energy Surface. MD simulations were performed for a set of 5 different total energy values. At the lowest total energies (with average temperatures below or equal to 300 K), the number of interconversions was not sufficient for convergence of the algorithm and the resulting isomer populations were strongly dependent on the starting geometry and should be taken with care. The system total energy was not high enough to enable frequent jumps over the potential energy barriers. At higher total energies (with average temperatures above 300 K), the five lowest energy minima were significantly populated while other structures were only negligibly adopted (the sum of their populations being less than 1%).

The global minimum Ip was always the most populated configuration and its population slightly decreased with increasing total energy. The population of the first local minimum remained almost constant during the total energy scan while the populations of the second and third local minima slightly increased with increasing total energy (see Figure 3). It may be of interest to note that, at all energies investigated, the glycine molecule with structure IVn is the second most abundant.

B. Glycine Dimer. *Experimental Results.* Mass Spectrometry. A mass spectrum recorded with the nozzle cooled to $T_0 = 12$ K is shown in Figure 4. It features major peaks on the masses $m = 4k$ amu belonging to ionized helium clusters and their fragments (He_k^+). Additional peaks appear at the masses $m =$ 30, 28, and 45 amu. They are assigned to the main fragmentation channels of the glycine molecule, $NH_2CH_2^+$, $(NH_2CH_2-2H)^+$, and $COOH^+$, respectively, arising from the cleavage of the C−C bond (see inset of Figure 4). Note that the signal on the glycine parent mass ($m = 75$ amu) is rather weak. Instead we observe rather strong signal for the protonated glycine molecule Gly·H^+ ($m = 76$ amu) and, with much lower intensity, also on the

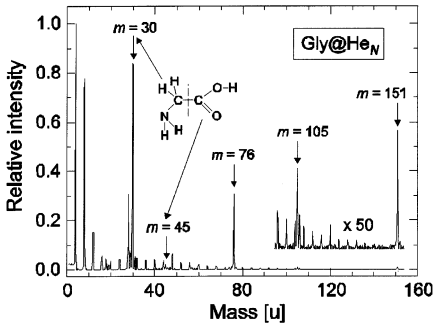

Figure 4. Mass spectrum of glycine trapped in liquid helium clusters. The temperature of the helium cluster source was $T_0 = 12$ K, yielding an average helium cluster size of $\langle N \rangle = 15\,000$. The glycine oven was heated to 120 °C.

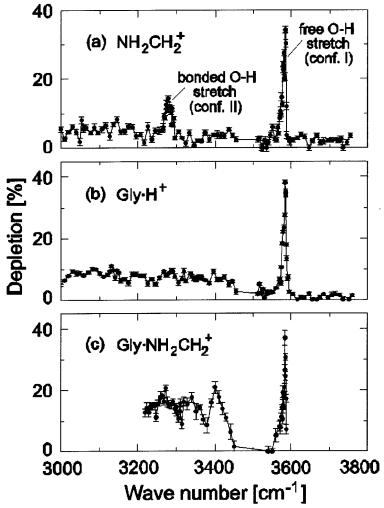

Figure 5. Infrared depletion spectra of glycine molecules and dimers trapped in liquid helium clusters as measured on various masses: $m =$ 30 amu ($NH_2CH_2^+$), $m = 76$ amu (Gly·H^+), and $m = 105$ amu (Gly·NH_2CH_2+). Spectra a and b were obtained with an original helium cluster size of $\langle N \rangle = 11\,000$. For recording spectrum c, the helium source was cooled to $T_0 = 12$ K, resulting in an average helium cluster size of $\langle N \rangle = 15\,000$.

masses $m = 105$ amu (Gly·NH_2CH_2+) and $m = 151$ amu (Gly$_2$·H^+). The mass peaks at $m = 76$ and 105 amu arise from glycine dimers embedded in helium clusters (Gly$_2$@He$_N$) or perhaps also from (fragmented) larger glycine complexes (Gly$_n$@He$_N$) while the signal on $m = 151$ amu is due to Gly complexes containing at least three glycine molecules. Mass spectra recorded at $T_0 = 14$ K and different temperatures of the glycine oven have already been published.[5] They feature significantly smaller signal on $m = 76$ amu and no signal on $m = 105$ and 151 amu.

IR Spectroscopy. Depletion spectra have been measured with the mass spectrometer tuned to $m = 30$ amu, the major monomer fragmentation channel, as well on $m = 76$ amu and $m = 105$ amu which are supposed to constitute the main dimer fragmentation channels. They are displayed in Figure 5. The uppermost spectrum shown in part a has already been discussed in a recent publication devoted to the IR spectroscopy of glycine molecules trapped in various rare gas matrixes and helium clusters.[5] This study revealed that the largest absorption peak at 3584.6 cm^{-1} must be attributed to the excitation of the (free) O−H stretch of glycine in its lowest energy conformer structure Ip (see Figure 1).

The second most intense absorption peak at 3274.7 cm^{-1} is assigned to glycine conformer II. This conformer is characterized

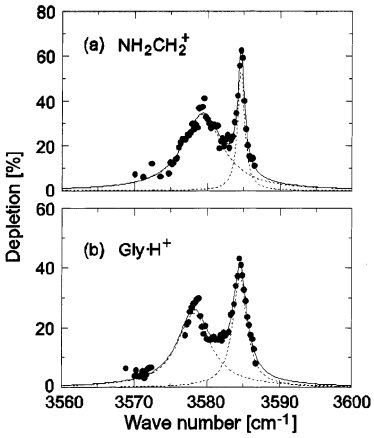

Figure 6. Infrared depletion spectra of glycine molecules and dimers trapped in liquid helium clusters as measured with a laser bandwidth of 0.2 cm^{-1}. The mass spectrometer was tuned to $m = 30$ amu (NH_2-CH_2^+) for spectrum a and $m = 76$ amu ($Gly{\cdot}H^+$) for spectrum b.

by an intramolecular hydrogen bond with the hydroxyl group pointing to the amino group. Due to the rather strong interaction, the O−H stretch is shifted by ∼310 cm^{-1} to the red (with respect to the free O−H stretch at ∼3585 cm^{-1}). The other two depletion spectra b and c cannot contain monomer absorption features since they were recorded on masses larger than the monomer mass; instead, they are assgined to the glycine dimer which fragments to $Gly{\cdot}H^+$ or $Gly{\cdot}NH_2CH_2^+$ when ionized. However, we cannot rule out the possibility that part of the signal observed on these masses stems from larger glycine complexes so that the absorption spectrum may contain contributions from Gly_n with $n > 2$. But this will not affect the essential result to be discussed here.

The spectra shown in Figure 5 have been obtained with a laser bandwidth of 2 cm^{-1}. To distinguish finer details in the free O−H absorption band, we have measured a 20 cm^{-1} wide region in the vicinity of the free O−H stretch with the highest possible resolution of our laser system which is 0.2 cm^{-1}. The result is shown in Figure 6. While the upper spectrum a, recorded with the mass spectrometer tuned to $m = 30$ amu, represents a monomer spectrum, the lower part b shows the result obtained for the dimer. Both spectra reveal a splitting into two bands at 3579.3 and 3584.6 cm^{-1}. In the earlier glycine monomer study, the lower frequency band was tentatively assigned to another conformer, namely, conformer III (see Figure 1). Surprisingly, the dimer spectrum resembles very much the monomer spectrum: the maximum positions coincide almost exactly, only the widths of the two bands are slightly different. This observation makes the earlier assignment somewhat doubtful.

The most interesting result of the present experimental study is the fact that the two dimer spectra measured on $m = 76$ and 105 amu feature a strong absorption band at 3585 cm^{-1}, at exactly the same position where the monomer free O−H stretch is observed. This unexpected result suggests that the major fraction of glycine dimers does not adopt the cyclic structure predicted by all earlier ab initio calculations. In these lowest energy structures the hydroxyl groups are engaged in a hydrogen bond which should give rise to an absorption band significantly shifted to the red (by 300 cm^{-1} or more) and no signal in the region of the free O−H stretch. From this it follows that the experiment is not compatible with a cyclic geometry as the only possible dimer structure.

One could argue that, under the conditions where the dimer spectrum b was measured, the helium clusters were contaminated by water molecules and that the signal on mass $m = 76$ amu could originate from fragmented $Gly{\cdot}H_2O$ complexes. While this is true, this argument does not hold for spectrum c of Figure 5 since the precursor of the $Gly{\cdot}NH_2CH_2^+$ ion must contain at least two glycine molecules. The absorption observed in spectrum c at 3400 cm^{-1} and below is ascribed to glycine complexes larger than the dimer. Note that spectrum c was measured at lower temperature than spectrum b and that, under the conditions of spectrum b, the signal on $m = 105$ amu was extremely poor. Although we have to admit that we do not understand all spectroscopic details, we have the clear experimental result that the free O−H stretch is rather strong in all spectra.

The structure of the global minimum of the glycine dimer was expected to have a planar cyclic arrangement with two strong O−H···O hydrogen bonds, which is analogous to the global minimum of the formic acid dimer.[25] Due to the existence of the strong O−H···O hydrogen bonds, both O−H stretching frequencies in this structure should be considerably shifted to the red. Surprisingly, the IR spectrum of the glycine dimer measured in helium droplets is only consistent with a structure having at least one free OH group not being involved in a hydrogen bond (see above). How can we interpret this finding? The only possibility is that the global minimum of the glycine dimer is not the cyclic H-bonded structure as was found for the formic acid dimer.[25] To answer this puzzle we utilize extended ab initio and MD analysis described below.

Computational Results. Potential Energy Surface. MD/Q searches with the empirical EP1 potential resulted in several hundred structures. The 22 lowest energy glycine dimer structures and their stabilization energies are shown in Figure 7 and Table 3, respectively. Surprisingly, the EP1 potential did not predict structure C1, characterized by a planar arrangement with two strong hydrogen bonds, as the global minimum but the stacked structure S1 (cf. Figure 7 and last column of Table 3); the energy difference between these two structures was as high as 3 kcal/mol. Furthermore even the first local minimum is a stacked structure (S2) and only the second local minimum is a planar one with two O−H···O hydrogen bonds. Higher-energy structures possess stacked, H-bonded (with one or two H-bonds) or T-shaped structures. All these geometries are energetically well separated from the global and first two local minima. Structures having the same pattern of H-bonds differ energetically less than structures with different H-bond patterns. Complexation behaviour of glycine is unexpected, if one considers the values of the acidity or basicity of the COOH and NH_2 groups. The gas-phase acidity of glycine is 342.5 kcal mol^{-1}, and the proton affinities of the NH_2 and COOH groups are 190 and 216 $kcal.mol^{-1}$, respectively.[26,27] One should therefore expect an interaction between the two COOH groups, leading to formation of homodimers, or between COOH group of one molecule and NH_2 of the other molecule, leading to formation of heterodimers.[6] Various structures of homo and heterodimers were detected using MD/Q technique (examples are shown in Figure 7), as well as dimers with different kind of geometrical arrangement. Comparing the stabilization energies (see Table 7) it is clear, that the most stable structures are C1 and S1. Therefore we inspected them in a more detailed way. Existence of stacked dimers is well-known in the case of nucleic acid base pairs and aromatic structures. In the present study we predicted for the first time an existence of a stacked structure for a compound without aromatic ring. The stabilization in stacked structures is mainly due to the dispersion energy, that plays a key role at distances about 3.0−3.5 Å. The S1 structure

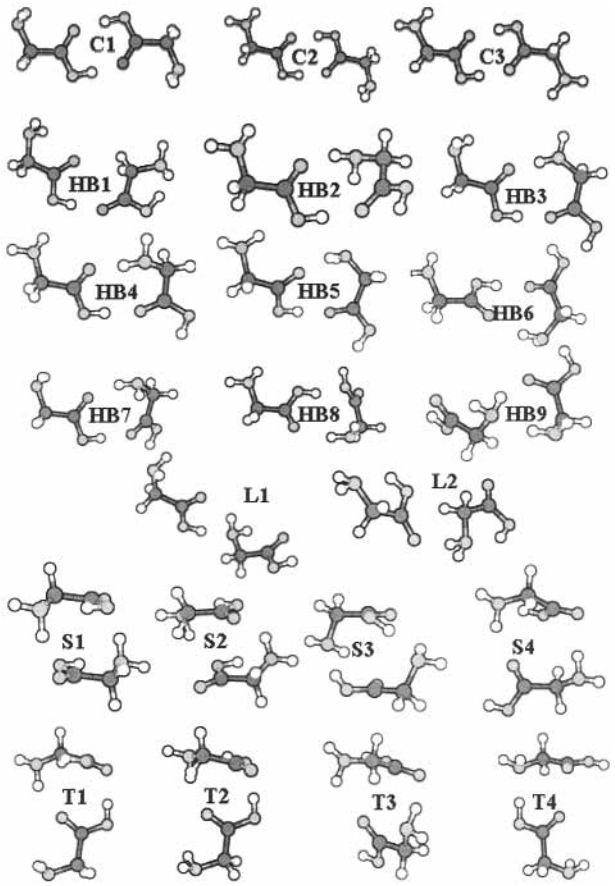

Figure 7. The 22 lowest energy structures of the glycine dimer as found by the MD/quenching/EP1 procedure.

TABLE 3: Relative Stabilization Energies (in kcal/mol) for the Lowest Energy Isomers of the Glycine Dimer

structure[a]	$\Delta\Delta E^{MP2/6-31G**}$	$\Delta\Delta E^{MP2/6-31G*(0.25)}$	$\Delta\Delta E^{EP1}$
C1	0.0	0.0	0.0
C2	−0.16	−0.108	−0.016
C3	−0.326	−0.222	0.017
S1	2.079	0.022	−2.976
S2	2.874	1.047	−1.810
S3	4.240	4.724	2.361
S4	6.490	4.625	2.836
HB1	4.117	3.262	3.391
HB2	4.127	4.641	4.583
HB3	4.889	4.033	3.610
HB4	4.969	4.104	3.517
HB5	5.805	4.667	4.353
HB6	5.786	4.390	4.581
HB7	5.943	4.175	4.200
HB8	8.120	6.824	7.286
HB9	9.363	7.943	8.095
T1	4.141	2.686	2.867
T2	4.669	3.219	2.572
T3	6.129	4.282	2.783
T4	2.147	2.276	5.385
L1	2.914	2.864	4.892
L2	7.550	6.814	6.070

[a] cf. Figure 7.

is formed in such a way that the glycine monomers are placed above each other keeping contacts between COOH and NH_2 groups of both monomers. The distance between carboxylic carbonyls is 3.0 Å. The additional stabilization (behind dispersion one) can be expected due to formation of hydrogen bonds between NH_2 and C═O groups (distance H···O is 2.2 Å). Comparing the geometry of C1 structure with analogous structure of formic acid dimer $[(Fo)_2]$ and acetic acid dimer $[(Ac)_2]$ (see Table 4) one can conclude that the present C1 structure does not differ from cyclic structures of $(Fo)_2$ and $(Ac)_2$ significantly. For detailed descriptions of $(Fo)_2$ and $(Ac)_2$ PES and FES see refs 25 and 28, respectively.

TABLE 4: H-bonded O...O Distances (in Angstroms) and Angles (in Degrees) in Planar Cyclic Structures of Formic Acid $[(Fo)_2]$, Acetic Acid $[(Ac)_2]$, and Glycine $[(Gly)_2]$ Dimers

	O(H)···O	C−O−H	O−C−O
$(Fo)_2$[a]	2.684	109.2	126.3
$(Ac)_2$[b]	2.671	109.1	123.9
$(Gly)_2$	2.667	109.3	124.4

[a] cf. ref 25. [b] cf. ref 28.

The only way to verify the empirical potential results is to recalculate the stabilization energies for all energy minima at the ab initio correlated level. The MP2 gradient optimization performed with the 6-31G** basis set (second column of Table 3) did not confirm the surprising result regarding the structure of the global minimum. As expected, the global minimum corresponded to the planar arrangement with two strong H-bonds. Also the first two local minima were cyclic H-bonded structures, and only the third local minimum was found to have a stacked structure. The energy difference between the planar H-bonded structures and the first stacked structure S1 is rather large (more than 2 kcal/mol). We are aware of the fact that the dispersion stabilization of the stacked structure S1 evaluated at the present theoretical level is underestimated, and therefore, the total stabilization energy of the stacked structure is also underestimated. Using the MP2/6-31G** dimer geometries, we determined the single point stabilization energy using a basis set containing more diffuse d-functions ($\alpha_d = 0.25$ instead of $\alpha_d = 0.8$ which is standardly used). This basis set (abbreviation 6-31G*(0.25)) is known to yield rather accurate stacking energies for DNA base pairs.[29] The resulting stabilization energies for all dimer structures are presented in Table 3 (third column). As expected, the energy difference between the C1 and S1 structures decreased from 2.1 kcal/mol to less than 0.1 kcal/mol. This means that both structures become now comparably stable. Furthermore, from inspection of Table 3, it is evident that the MP2/6-31G*(0.25) relative stabilization energies are closer to the relative energies obtained with the empirical EP1 potential. While the MP2/6-31G*(0.25) calculations give comparable stability for the C1 and S1 structures, the EP1 potential prefers the stacked structure over the planar structure by about 3 kcal/mol. Is this an artifact of the empirical potential or does it reflect the physical reality? To answer this question, we performed the following higher level computations:

(i) Using a larger basis set (aug-cc-pVDZ, containing diffuse s, p, and d functions), we performed the gradient optimization for the structures C1 and S1. The resulting stabilization energies are presented in Table 5. Before introducing the a posteriori BSSE corrections, the stabilization energies of both structures were comparable. After considering the BSSE, the C1 structure became slightly more stable (by 1.3 kcal/mol). Passing from the MP2/6-31G** to the MP2/aug-cc-pVDZ description (gradient optimization + a posteriori BSSE), the relative stability of the S1 structure with respect to the C1 structure was improved by 0.8 kcal/mol. Improving the basis set further, we can thus expect a further decrease of the stabilization energy difference between both structures. To prove this conjecture, we performed MP2/aug-cc-pVTZ single point calculations of the stabilization energies for the MP2/aug-cc-pVDZ optimized C1 and S1 geometries. Table 6 shows that this step leads to a slight stability increase of C1 relative to S1. The MP2/aug-cc-pVDZ calcula-

TABLE 5: Comparison of the Relative Energies (in kcal/mol) of the C1 and S1 Structures Calculated at Different ab Initio Levels[a]

structure	ΔE^C	$\Delta E(1)$	$\Delta E(2)$	$\Delta E(3)$	$\Delta E(4)$	$\Delta E(5)$	ΔE^{CP}	ΔH_0^0
C1	0.000	0.000	0.000	0.000	0.000	0.000	0.000	0.000
S1	−2.976	2.079	0.022	1.285	1.734	1.536	1.695	2.079

[a] ΔE^C: relative energies calculated using the empirical potential of Cornell et al. $\Delta E(1)$: MP2/6-31G**//MP2/6-31G**; BSSE a posteriori. $\Delta E(2)$: MP2/6-31G*(0.25)//MP2/6-31G**; BSSE a posteriori. $\Delta E(3)$: MP2/aug-cc-pVDZ//MP2/aug-cc-pVDZ; BSSE a posteriori. $\Delta E(4)$: MP2/aug-cc-pVTZ//MP2/aug-cc-pVDZ; BSSE a posteriori. $\Delta E(5)$: RI-MP2/TZVPP//RI-MP2/TZVPP; BSSE a posteriori. ΔE^{CP}: CP optimization at MP2/6-31G** level. ΔH_0^0: ΔZPVE at MP2/6-31G** level included.

TABLE 6: Relative Stabilization Energies (in kcal/mol) of the C1 and S1 Structures Evaluated at Different ab Initio Levels for Geometries Optimized at the MP2/aug-cc-pVDZ Level[a]

structure	$\Delta E(1)$	$\Delta E(2)$	$\Delta E(3)^b$	$\Delta E(4)$
C1	0.000	0.000	0.000	0.000
S1	−0.217	0.866	0.009	0.300

[a] $\Delta E(1)$: MP2/6-31G*(0.25)//MP2/aug-cc-pVDZ; BSSE a posteriori. $\Delta E(2)$: CCSD/6-31G*(0.25)//MP2/aug-cc-pVDZ; BSSE a posteriori. $\Delta E(3)$: CCSD(T)/6-31G*(0.25)//MP2/aug-cc-pVDZ; BSSE a posteriori. $\Delta E(4)$: QCISD(T)/6-31G*(0.25)//MP2/aug-cc-pVDZ; BSSE a posteriori. [b] BSSE for the S1 structure was estimated at the CCSD level because it was not possible to perform this calculation at the CCSD(T) level due to the large requirements on memory and disk space.

tions yield very good stabilization energies but their performance for evaluation of the structure of a dimer could be lower. We performed therefore the RI-MP2/TZVPP optimizations (the basis set used contains f-functions on heavy atoms and d-functions on hydrogens). From Table 5 it is evident that these calculations did not bring any significant differences when compared with the MP2 results.

(ii) The role of higher correlation energy contributions was further investigated using MP2/aug-cc-pVDZ geometries of the C1 and S1 structures. The respective relative stabilization energies are collected in Table 6. For the sake of comparison, we first performed the MP2/6-31G**(0.25) calculations which gave a slightly preferential stability for the stacked structure S1. The CCSD calculations with the same basis set gave opposite results, the C1 structure being now preferred. Considering, however, the triple excitations, the energy difference between C1 and S1 was again reduced.

Another source of inaccuracy is included in the way of gradient optimization. All above-mentioned results were obtained for geometries determined by standard gradient optimization. The more physical CP-corrected gradient optimization yields different geometries for both structures investigated and thus yields different stabilization energies. The CP-corrected gradient optimization was performed at the MP2/6-31G** level for the C1 and S1 structures, and the respective stabilization energies are presented in Table 5. It is found that the CP-corrected optimization reduces the energy difference between the S1 and C1 structures from 2.1 to 1.7 kcal/mol, i.e., by 0.4 kcal/mol. This means that the theoretically more justified CP-corrected gradient optimization reduces the difference between the planar and stacked structures and this reduction will be larger for the basis sets possessing a larger value of BSSE. Thus, we can expect that the CP-corrected optimization performed at the MP2/aug-cc-pVDZ level will lower the existing difference between the C1 and S1 structures (1.3 kcal/mol) by more than 0.4 kcal/mol.

TABLE 7: MP2/6-31G O−H and N−H Symmetric (S) and Antisymmetric (A) Harmonic Stretching Frequencies of the Glycine Dimer (D) and Corresponding Monomer (M) in cm^{-1} Calculated at the MP2/6-31G** Level (All values Scaled by the Factor 0.943)**

structure	M[a]	D(S)[a]	D(A)[a]	M(S)[b]	M(A)[b]	D(S)[b]	D(A)[b]
C1	3596	3084	3175	3375	3463	3380	3468
S1	3366	3218	3227	3381	3495	3381	3481
T4	3595	2879[c]	3603[d]	3385	3487	3370	3468[e]
						3368	3456[f]

[a] OH stretch. [b] NH stretch. [c] H-bonded O−H stretch. [d] Free O−H stretch. [e] H-bonded NH_2 stretch. [f] Free NH_2 stretch.

The role of zero-point energy correction was investigated at the MP2/6-31G** level. From Table 5, however, it is obvious that the ΔZPVE does not change the relative energies between the S1 and C1 structures.

Taking all these effects into account and extrapolating them, we must conclude that, with increasing level of the ab initio calculations, the structures C1 and S1 become comparably stable or the stacked structure S1 becomes even slightly more stable. This rather surprising result thus fully confirms the prediction of the empirical EP1 potential about the higher stability of the stacked structure S1.

The finding that the stacked structure S1 might coexist with the H-bonded planar structure C1 still does not explain the experimental result that the glycine dimer possesses free OH groups which are not H-bonded. According to the calculations, the stacked structure S1 is composed of two glycine molecules of conformer II. This means that they have an intramolecular hydrogen bond that should give rise to a red shift for the O−H stretch of approximately 300 cm^{-1} as observed for the monomer (see Figure 5a). However, it could be that this red shift is somewhat reduced due to the intermolecular interactions that weaken the intramolecular H-bond.

A closer look at Figure 7 reveals that, from the 22 lowest-energy structures, only the structures S4, HB2−HB9, L1, and T1−T4 have at least one free (non-hydrogen-bonded) OH group. However, these structures have stabilization energies that are at least 2.5 kcal/mol higher than that of the C1 isomer (for the empirical potential). This energy difference is even larger if the ab initio calculations are used. To investigate all possibilities, we have also performed higher level calculations for the T4 structure. For $\Delta E(3)$ and ΔE^{CP} (see Table 4 for notation) we obtained values of 2.529 and 2.157 kcal/mol, respectively. Since these values are not much larger than those for C1 and S1 it follows that the T4 structure could be adopted at higher temperature. Under the experimental conditions of the present study, however, this is unlikely. Finally, higher level calculations carried out for the structures T1, HB1, and S4, yielded energies that were between 1.2 and 2.9 kcal/mol higher than for the T4 structure (at the $\Delta E(3)$ level).

Vibrational Spectra. The O−H stretching frequencies of the C1 and S1 structures were calculated at the harmonic MP2/6-31G** level. The wavenumber values, that were scaled by the recommended factor[30] of 0.943, are presented in Table 7. The O−H stretching frequency of the Ip monomer (3596 cm^{-1}) agrees very well with the experimental value (3585 cm^{-1}; cf. Figure 5) which gives us confidence in our vibrational frequency calculation. From the table, it follows that the O−H stretches of the dimer in the C1 structure are red-shifted by 421 and 512 cm^{-1} (asymmetric and symmetric vibrations) with respect to the monomer O−H vibration. Due to the anharmonic coupling, these shifts represent a lower limit of the real shifts. In our

previous paper on the glycine monomer,[31] we have shown that the O−H stretch in the first local minimum (having an intramolecular hydrogen bond) is red-shifted by 230 cm^{-1} with respect to the free O−H stretch of the global minimum monomer. Considering, however, all anharmonic couplings, this shift increases to 360 cm^{-1} which is very close to the experimental value[5] of 310 cm^{-1}. Scaling to this experimental value and multiplying the calculated red shift of the infrared-active asymmetric stretch of the cyclic dimer C1 by the factor 310/230, we obtain a rather realistic estimate of the true dimer shift (567 cm^{-1}). This locates the IR-active O−H stretch of the C1 dimer at 3029 cm^{-1}, close to the lower-frequency edge of the experimental spectrum.

The situation with the stacked structure S1 is similar. From Table 7 it follows that the O−H stretch (D(A)) in this structure is red-shifted by 369 cm^{-1} with respect to the free O−H stretch of monomer I (3596 cm^{-1}). Applying the same correction to account for the anharmonic coupling, the red shift increases by the factor 310/230, thus positioning the asymmetric stretch of the glycine dimer in the S1 structure at 3099 cm^{-1}.

The calculated vibrational spectra also give evidence of the formation of a weak intermolecular N−H···O hydrogen bond in the S1 dimer structure. The asymmetric N−H stretching frequency is red-shifted by 14 cm^{-1} with respect to the same vibration in the free IIn monomer. Note that the shifts of the N−H stretches in the planar C1 structure are only 5 cm^{-1} and go to higher frequencies. The only dimer with a free OH group was found to be the T4 structure, and to some extend also the T3 structure. The H-bonded O−H stretching frequency is located at 2879 cm^{-1} giving rise to an extremely large red shift of 717 cm^{-1}, which is even larger than the ones for the structures C1 and S1. Evidently, this band is far from the spectral range accessed in the present experiment.

We conclude this section by stating that the calculated hydrogen-bonded O−H stretches of the C1 and S1 structures are strongly red-shifted with respect to the free O−H stretch of the glycine monomer in the global minimum Ip. The estimated shifts are 560 cm^{-1} for the planar cyclic C1 structure and close to 500 cm^{-1} for the S1 sandwich structure. Thus, theory locates these vibrations close to 3000 cm^{-1} or perhaps below. Since the measured spectrum starts at 3000 cm^{-1} it could be that these vibrations have escaped experimental observation. However, it is difficult to believe that a *strong* vibrational band located between 2900 and 3000 cm^{-1} will not be seen at 3000 cm^{-1}. On the other hand, we have the experimental observation of a strong dimer O−H stretch close to the monomer vibration. This indicates that the corresponding OH group is not engaged in a hydrogen bond. The only dimer geometry featuring a free OH group is the T-shaped T4 structure.

Its stabilization energy is rather high so that a significant population of this structure can be ruled out in a system well-equilibrated at the present temperature of 0.4 K. In the helium droplet, however, the molecular system may not necessarily have time to properly equilibrate. As revealed by our MD simulations, the interconversion rate for glycine dimer is rather low for temperatures below 400 K. The observed time scale for transition between isomers is in the nanosecond range. On the other hand, the cool down of the glycine molecule inside the helium droplet is estimated to happen in less than a nanosecond. It can therefore be expected to observe also higher energy structures, such as isomer T4 with a free OH group, in the present droplets as the local minimum structure may be frozen quickly and thus preserved because the system does not have enough time to properly equilibrate.

TABLE 8: Empirical Interaction Energies (ΔE^{EP1}) for 17 Structures Populated by More than 1% at a Constant Total Energy of 77.1 kcal/kol and Their Relative Populations (pop) at Constant Total Energies of 66.2, 71.3, 77.1, 82.9, and 88.5 Kcal/Mol (in %)

MD total energy: structure[a]	ΔE^{EP1}	66.2 pop	71.3 pop	77.1 pop	82.9 pop	88.5 pop
C1	−16.445	12.8	15.6	7.6	6.0	2.6
C2	−16.461	12.2	15	8.0	6.4	3.5
C3	−16.428	1.3	1.7	0.9	0.7	0.4
C4	−16.304	1.2	1.5	0.8	0.7	0.3
C5	−15.948	4.1	5.0	3.1	2.5	1.5
C6	−15.898	0.9	1.0	0.7	0.8	0.3
C7	−15.792	0.8	1.0	0.6	0.5	0.3
S1	−19.421	2.3	2.5	1.3	0.9	0.3
S2	−18.255	2.0	1.6	1.1	0.8	0.4
HB1	−13.056	2.1	2.4	2.1	2.0	1.3
HB2	−11.862	1.9	1.9	2.0	2.0	1.8
HB4	−12.928	2.1	2.3	2.2	2.3	1.6
HB5	−12.092	0.9	1.0	1.1	1.0	0.9
HB7	−12.245	5.0	5.0	5.2	4.7	3.2
T1	−13.578	2.2	2.5	1.1	1.6	0.9
T2	−13.873	1.2	1.3	5.2	1.1	0.9
L1	−11.573	2.9	2.7	1.7	2.8	2.2

[a] cf. Figure 7.

It can also be possible that the glycine dimer global minimum structure adopted in helium droplets differs from that in the gas phase which is simulated by the theory. As has been shown in the previous sections, the global minimum of the glycine dimer is rather shallow and, depending on the level of theory, different (and even very different) dimer structures are favored. Taking into account the additional interaction of the two glycine molecules with the helium atoms, one could imagine that this may lead to structures different from those given here. Unfortunately, it is beyond the capability of current computers to fully account for the interaction with the helium droplet. Finally, it should be mentioned that, for other systems, it has already been observed that the structures of hydrogen-bonded complexes may be different if they are formed in helium droplets. Examples include the HCN trimer and larger complexes of HCN that have been found to adopt linear chains in helium droplets[32] (in contrast to cyclic structures in the gas phase) and the water hexamer which has a planar cyclic geometry in helium[33] but a three-dimensional prisme-shaped structure in the free gas phase. These phenomena are most probably due to the nature of the cooling process.

Free Energy Surface. Albeit irrelevant to the present low-temperature experiment, we have carried out long runs of MD simulations to determine the populations of various dimer structures. At a total energy of 77.1 kcal/mol (corresponding to an average temperature of 300 K) 48 structures and at a total energy of 88.5 kcal/mol (corresponding to an average temperature of 400 K) even 66 structures were populated with populations higher than 0.3%. From these configurations, we chose 22 structures representing various arrangements of the general geometric motif and evaluated their stabilization energies at the MP2/6-31G**/6-31G(0.25)//MP2/3-31G** ab initio level to check the quality of the empirical potential (see Table 3).

The temperature dependence of the populations of 17 structures, for which the population was greater than or equal to 1% at 300 K, is given in Table 8 and in Figure 8. Evidently, entropy strongly favors the cyclic structures C1 and C2 and disfavors all stacked structures. The populations of C1 and C2 slightly decrease with increasing temperature while more stuctures become important and the populations are spread out. The differences between their populations are rather small. A

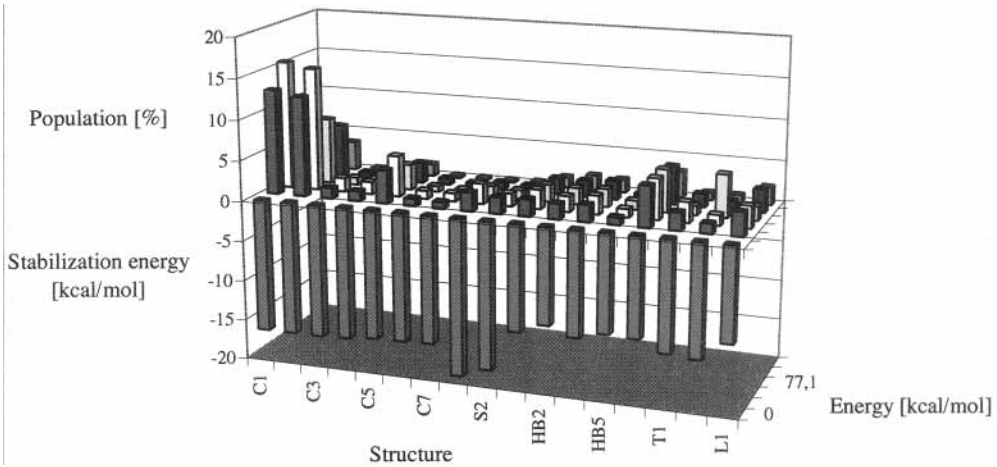

Figure 8. Three-dimensional histogram of relative populations of the glycine dimer isomers (cf. Figure 7) for the following values of the MD total energy E^{tot} = 66.2, 71.3, 77.1, 82.9, and 88.5 kcal/mol (cf. also Table 7).

similar effect has been observed previously[25] for the formic acid dimer where the highest population at low temperature (~100 K) was found for the expected cyclic structure with two hydrogen bonds while, at higher temperature (~300 K), the highest population was calculated for an energetically less stable structure corresponding to the first local minimum.

V. Conclusion

The essential results of the present combined theoretical and experimental efforts can be summarized as follows:

1. The calculations performed with the empirical EP1 potential predict the sandwich structure S1 to be more stable than the planar cyclic structure C1 with two strong O−H···O hydrogen bonds.

2. On the other hand, the correlated ab initio calculations (MP2/6-31G**) prefers structure C1 over S1. After extending the basis set, improving the optimization, and covering the large portion of electron correlation, comparable stabilization energies for both structures (C1 and S1) are obtained.

3. High-level correlated calculations also reveal that the T-shaped structure T4 with one free and one bonded OH group is only 1−2 kcal/mol less stable than the structures C1 and S1.

4. The O−H stretching vibrations of the most important dimer structures are calculated within the harmonic approximation. For the lowest energy structures C1 and S1, rather large red shifts (360−420 cm^{-1}) are obtained. This is because all OH groups are hydrogen-bonded (intermolecular H-bond for C1 and intramolecular H-bond for S1). Estimation of the effect of anharmonicity locates these vibrations close to or just below 3000 cm^{-1}, the lower limit of the frequency range accessed by the present experiment.

5. The experimental glycine dimer spectra feature a strong vibrational band at the same position where the free O−H stretch of the monomer is observed. While the bonded O−H stretches will escape experimental observation if they fall below 3000 cm^{-1} the observation of the free O−H stretch can be explained by the fast (time scale < ns) cooling process inside the helium droplet. The glycine dimer thus freezes in its local minimum geometry which may be a T-shaped structure, for example, structure T4.

6. Another possible explanation of the experimental spectrum is that the glycine dimer in liquid helium droplets adopts different global minimum structure (for example T4) than in the gas phase. A similar behavior has already been observed for other hydrogen-bonded systems but most probably is again due to the cooling process rather than a change the global minimum geometry.

7. Finally and for curiosity, it should be mentioned that the experimental observation of the free O−H stretching vibration has questioned the classical cyclic dimer structure C1 and has prompted the ambition of theoreticians to find another dimer structure of higher or at least comparable stability. This search was successful and uncovered the new stacked structure S1.

Acknowledgment. F.H. and O.W. are grateful to the Deutsche Forschungsgemeinschaft for financial support within the Schwerpunktprogramm *Molecular Clusters*. This project, LN 00A032 (Center for Complex Molecular Systems and Biomolecules), was supported by the Ministry of Education of the Czech Republic. The authors also gratefully acknowledge CPU time on the NEC-SX4 at CHMI Prague (Grant no. LB 98202, project Infra2 of MŠMT ČR).

References and Notes

(1) Császár, A. G. *J. Am. Chem. Soc.* **1992**, *114*, 9568.
(2) Alexandrov, V.; Stepanian, S.; Adamovicz, L. *Chem. Phys. Lett.* **1998**, *291*, 110.
(3) Neville, J. J.; Zheng, Y.; Brion, C. E. *J. Am. Chem. Soc.* **1996**, *118*, 10533.
(4) Stepanian, F.; Reva, I. D.; Radchenko, E. D.; Rosado, M. T. S.; Duarte, M. L. T. S.; Fausto, R.; Adamovitz, L. *J. Phys. Chem.* **1998**, *102*, 1041.
(5) Huisken, F.; Werhahn, O.; Ivanov, A. Yu.; Krasnokutski, J. A. *J. Chem. Phys.* **1999**, *111*, 2978.
(6) De Wael, K.; Zeegers-Huyskens, T. *Biopolymers* **1997**, *41*, 205.
(7) Amar, F. G.; Berry, R. S. *J. Chem. Phys.* **1986**, *85*, 5943. Stillinger, F. M., Weber, T. A. *Phys. Rev.* **1982**, *A23*, 987. Vacek, J.; Hobza, P. *J. Phys. Chem.* **1995**, *99*, 17088.
(8) Cornell, W. D.; Cieplak, P.; Bayly, C. I.; Gould, I. R.; Merz, K. M.; Ferguson, D. M.; Spellmeyer, D. C.; Fox, T.; Caldwell, J. E.; Kollman, P. *J. Am. Chem. Soc.* **1995**, *117*, 5179.
(9) Kratochvíl, M.; Enkvist, O.; Šponer, J.; Jungwirth, P.; Hobza, P. *J. Phys. Chem.* **1998**, *102*, 6921.
(10) Feyrereisen, M.; Fitzgerald, G.; Komornicki, A. *Chem. Phys. Lett.* **1993**, *208*, 359.
(11) Vahtras, O.; Almlöf, J.; Feyereisen, M. *Chem. Phys. Lett.* **1993**, *213*, 514.
(12) Bernholdt, D. E.; Harrison, R. J. *Chem. Phys. Lett.* **1996**, *250*, 470.
(13) Boys, S. B.; Bernardi, F. *Mol. Phys.* **1970**, *19*, 553.
(14) Simon, S.; Duran, M.; Dannenberg, J. J. *J. Chem. Phys.* **1996**, *105*, 11024.
(15) Hobza, P.; Havlas, Z. *Theor. Chem. Acc.* **1998**, *99*, 372.
(16) Frisch, M. J.; Trucks, G. W.; Schlegel, H. B.; Scuseria, G. E.; Robb, M. A.; Cheeseman, J. R.; Zakrzewski, V. G.; Montgomery, J. A., Jr.; Stratmann, R. E.; Burant, J. C.; Dapprich, S.; Millam, J. M.; Daniels, A. D.; Kudin, K. N.; Strain, M. C.; Farkas, O.; Tomasi, J.; Barone, V.; Cossi, M.; Cammi, R.; Mennucci, B.; Pomelli, C.; Adamo, C.; Clifford, S.; Ochterski, J.; Petersson, G. A.; Ayala, P. Y.; Cui, Q.; Morokuma, K.; Malick, D. K.; Rabuck, A. D.; Raghavachari, K.; Foresman, J. B.; Cioslowski, J.;

Ortiz, J. V.; Stefanov, B. B.; Liu, G.; Liashenko, A.; Piskorz, P.; Komaromi, I.; Gomperts, R.; Martin, R. L.; Fox, D. J.; Keith, T.; Al-Laham, M. A.; Peng, C. Y.; Nanayakkara, A.; Gonzalez, C.; Challacombe, M.; Gill, P. M. W.; Johnson, B. G.; Chen, W.; Wong, M. W.; Andres, J. L.; Head-Gordon, M.; Replogle, E. S.; Pople, J. A. *Gaussian 98*, revision A.7; Gaussian, Inc.: Pittsburgh, PA, 1998.

(17) Allrichs, R.; Bär, M.; Häser, M.; Horn, H.; Kölmel, C. *Chem. Phys. Lett.* **1989**, *162*, 165.

(18) Applequist, J. *Acc. Chem. Res.* **1977**, *10*, 79.

(19) Bayly, C. I.; Cieplak, P.; Cornell, W. D.; Kollman, P. *J. Phys. Chem.* **1993**, *97*, 10269.

(20) Cornell, W. D.; Cieplak, P.; Bayly, C. I.; Kollman, P. *J. Am. Chem. Soc.* **1993**, *115*, 9620.

(21) Weiner, P. K.; Kollman P. A. *J. Comput. Chem.* **1981**, *3*, 287.

(22) Fröchtenicht, R.; Kaloudis, M.; Koch, M.; Huisken, F. *J. Chem. Phys.* **1996**, *105*, 6128.

(23) Hartmann, M.; Miller, R. E.; Toennies, J. P.; Vilesov, A. *Phys. Rev. Lett.* **1995**, *75*, 1566.

(24) Huisken, F.; Kulcke, A.; Voelkel, D.; Laush, C.; Lisy, J. M. *Appl. Phys. Lett.* **1993**, *62*, 805.

(25) Chocholoušová, J.; Vacek, J.; Hobza, P. *Phys. Chem. Chem. Phys.* **2002**, *4*, 2119.

(26) Slaughter, A. R.; Banna, M. S. *J. Phys. Chem.* **1988**, *92*, 2165.

(27) Meot-Ner, M *J. Am. Chem. Soc.* **1988**, *110*, 3071.

(28) Chocholoušová, J.; Vacek, J.; Hobza, P. In prepation.

(29) Hobza, P. Šponer, J. *Chem. Rev.* **1999**, *99*, 3247.

(30) Scheiner, S. *Hydrogen Bonding*; Oxford University Press: New York, 1997.

(31) Bludský, O.; Chocholoušová, J.; Vacek, J.; Huisken, F.; Hobza, P. *J. Chem. Phys.* **2000**, *113*, 4629.

(32) Nauta, K.; Miller, R. E. *Science* **1999**, *283*, 1895.

(33) Nauta, K.; Miller, R. E. *Science* **2000**, *287*, 293.